Geophysical Research Letters

RESEARCH LETTER
10.1029/2019GL083657

The Record-Setting 2018 Eastern North Pacific Hurricane Season

Kimberly M. Wood[1], Philip J. Klotzbach[2], Jennifer M. Collins[3], and Carl J. Schreck[4]

[1]Department of Geosciences, Mississippi State University, Mississippi State, MS, USA, [2]Department of Atmospheric Science, Colorado State University, Fort Collins, CO, USA, [3]School of Geosciences, University of South Florida, Tampa, FL, USA, [4]Cooperative Institute for Climate and Satellites – NC (CICS-NC), North Carolina State University, Asheville, NC, USA

Key Points:
- The eastern North Pacific set records for hurricane activity in 2018 with relatively little influence from El Niño-Southern Oscillation
- Combined above (below)-average sea surface temperatures and moisture (shear) during August and September contributed to the record season
- The strongly positive Pacific Meridional Mode also supported the increase in eastern North Pacific hurricane activity

Supporting Information:
- Supporting Information S1

Correspondence to:
K. M. Wood,
kimberly.wood@msstate.edu

Citation:
Wood, K. M., Klotzbach, P. J., Collins, J. M., & Schreck, C. J. (2019). The Record-Setting 2018 Eastern North Pacific Hurricane Season. *Geophysical Research Letters*, *46*, 10,072–10,081. https://doi.org/10.1029/2019GL083657

Received 10 MAY 2019
Accepted 6 AUG 2019
Accepted article online 9 AUG 2019
Published online 21 AUG 2019

Abstract The extremely active 2018 eastern North Pacific (ENP) hurricane season set records for number of hurricane days, major hurricane days, and accumulated cyclone energy (ACE). The Western Development Region (116°W–180°) was especially active, shattering its prior record for ACE set in 2015. In addition, Hawaii was impacted by Hurricane Lane in August and Tropical Storm Olivia in September. Despite above-normal sea surface temperatures (SSTs) and below-normal vertical wind shear in 2018, large-scale conditions were generally less conducive for tropical cyclone (TC) formation than in 2015. However, the strong subtropical ridge in August and September of 2018 enhanced westward steering flow, thereby keeping TCs over hurricane-favorable conditions and preventing recurvature toward lower SSTs and higher vertical wind shear. The 2018 ENP hurricane season highlights that El Niño conditions are not necessary for extremely high ENP TC activity.

Plain Language Summary The 2018 eastern North Pacific hurricane season broke records, particularly when considering an index that accounts for frequency, intensity, and duration of hurricanes. The previous record was set in 2015 during a strong El Niño event that increased ocean warmth and thus provided more fuel for hurricanes. Even though a weak El Niño did not develop until late in the 2018 hurricane season, the ocean was warmer than normal in the region where the hurricanes formed, which helped support their development. After the hurricanes formed, the flow of the atmosphere generally kept them over warmer water, helping them last longer. We need to study more seasons like 2018 to better understand when eastern North Pacific hurricane seasons will be active without the presence of a strong El Niño.

1. Introduction

The 2018 eastern North Pacific (ENP) hurricane season generated 318 × 10^4 kt^2 of accumulated cyclone energy (ACE; Bell et al., 2000), more than any other season since 1971 (the beginning of the reliable satellite era; Blake et al., 2009). This record-breaking season began with El Niño-Southern Oscillation (ENSO) in a neutral state. Several studies have noted a weak-to-nonexistent relationship between ENP tropical cyclone (TC) frequency and ENSO (e.g., Whitney & Hobgood, 1997). However, the *location* of TC activity appears to change with ENSO phase. Westward shifts in TC genesis and track are associated with El Niño events (e.g., Camargo et al., 2008; Irwin & Davis, 1999). More conducive environmental conditions in the western ENP likely contribute to this westward shift, particularly west of 116°W (Collins & Mason, 2000). Warm ENSO conditions also favor higher ACE (Collins et al., 2016), and TC activity increases in the western ENP during El Niño years compared to La Niña years (Jien et al., 2015).

Beyond ENSO, positive phases of the Pacific Decadal Oscillation (PDO) are associated with more frequent impacts in Mexico and the southwest United States due to ENP TC landfall and/or TC-related moisture moving inland (Raga et al., 2013; Wood & Ritchie, 2013). The positive phase of the Atlantic Multidecadal Oscillation (AMO) may suppress ENP TC activity by strengthening upper-level easterly winds and thus vertical wind shear over the eastern part of the basin (Wang & Lee, 2009). A negative phase of the AMO —associated with a colder North Atlantic gyre—can lead to more ENP activity (Caron et al., 2015). Overall, changes in thermodynamic conditions over the North Atlantic related to the AMO and the

Atlantic Meridional Mode (Chiang & Vimont, 2004) affect dynamic conditions over the ENP (Caron et al., 2015; Patricola et al., 2017; Smith et al., 2010). The Pacific Meridional Mode (PMM; Chiang & Vimont, 2004) may have influenced the active 2015 ENP hurricane season (Collins et al., 2016), but a climatological assessment of the PMM's influence in the ENP has yet to be performed.

During 2018, several ENP TCs significantly impacted land. In October, Hurricane Willa made landfall in Sinaloa, Mexico, with an estimated intensity of 105 kt and caused over $500 million (2018 USD) in damage, making it the sixth-costliest hurricane on record in Mexico (Brennan, 2019). Hurricane Lane affected Hawaii in August, bringing up to 58″ of rain to the eastern part of the Big Island (https://www.wpc.ncep.noaa.gov/tropical/rain/lane2018.html). The following month, Tropical Storm Olivia made landfall in Maui, the island's first TC landfall since at least 1949 based on the second-generation Hurricane Best Track dataset (HURDAT2; Landsea & Franklin, 2013).

In contrast to 2018, the hyperactive season of 2015 occurred during a near record-strength El Niño event and produced the most intense ENP TC on record (Hurricane Patricia). The strong 2015 El Niño contributed to the most TC-favorable conditions in the past 30 years west of 116°W: the highest sea surface temperatures (SSTs), the highest total precipitable water, and the lowest 200-850-hPa vertical wind shear (Collins et al., 2016).

This study focuses on the level and distribution of TC activity west of 116°W during the 2018 ENP hurricane season and then diagnoses environmental factors contributing to the high levels of observed TC activity. We then contrast conditions between the 2018 and 2015 hurricane seasons and evaluate the role of large-scale variability to provide further insight for future hyperactive seasons.

2. Data and Methods

We calculate ACE and other metrics of TC activity (named storm days, hurricane days, and major hurricane days) from the 1 July 2019 update of HURDAT2. For Walaka (2018), we use the operational best track (http://hurricanes.ral.ucar.edu/repository/data/bdecks_open/). Our 2015 TC metrics differ slightly from those presented in Collins et al. (2016) because we use HURDAT2 rather than the operational best tracks available at the time of the previous study.

In this study, we investigate TC activity from 1988 to 2017, the most recent 30-year period, as a baseline for 2018 activity. The National Hurricane Center took operational responsibility for the ENP from 140°W to the coast of North America in 1988 (Klotzbach & Landsea, 2015), thus providing a reliable, contiguous record from a single warning agency east of 140°W.

We evaluate atmospheric fields using the 6-hourly, ~0.7° spatial resolution (T255 spectral resolution) European Centre for Medium-range Weather Forecasts Interim Reanalysis (ERA-Interim; Dee et al., 2011). ERA-Interim fields are obtained from the University Corporation for Atmospheric Research Data Archive (https://rda.ucar.edu/). ERA-Interim supplies most fields except vertical wind shear, calculated as the vector wind difference between 200 and 850 hPa. We also evaluate daily, 0.25° SST from the National Oceanic and Atmospheric Administration optimum interpolation dataset (OISST; https://www.esrl.noaa.gov/psd/data/gridded/data.noaa.oisst.v2.highres.html).

To investigate the relationship between large-scale climate variability and ENP TC activity during 1988–2018, we quantify ENSO phase with the Oceanic Niño Index (https://www.esrl.noaa.gov/psd/data/correlation/oni.data) and the Multivariate ENSO Index (Wolter & Timlin, 1998). We also examine the PMM (Chiang & Vimont, 2004) and the PDO (Mantua et al., 1997; https://www.ncdc.noaa.gov/teleconnections/pdo/). In addition, we assess the ability of a two-predictor diagnostic model (Caron et al., 2015) to forecast the record-breaking 2018 ENP hurricane season.

Impacts of the Madden-Julian oscillation (MJO) and convectively coupled Kelvin waves are identified using a wavenumber-frequency Fourier filter of outgoing longwave radiation (Schreck et al., 2018) and ERA-Interim 850-hPa zonal wind. The Kelvin wave filter follows Kiladis et al. (2009), and the MJO filter follows Kiladis et al. (2005). Both fields are shown as Hovmöllers for 5–15°N to correspond with the latitudes of maximum variance in these fields over the ENP (Kiladis et al., 2005, 2009).

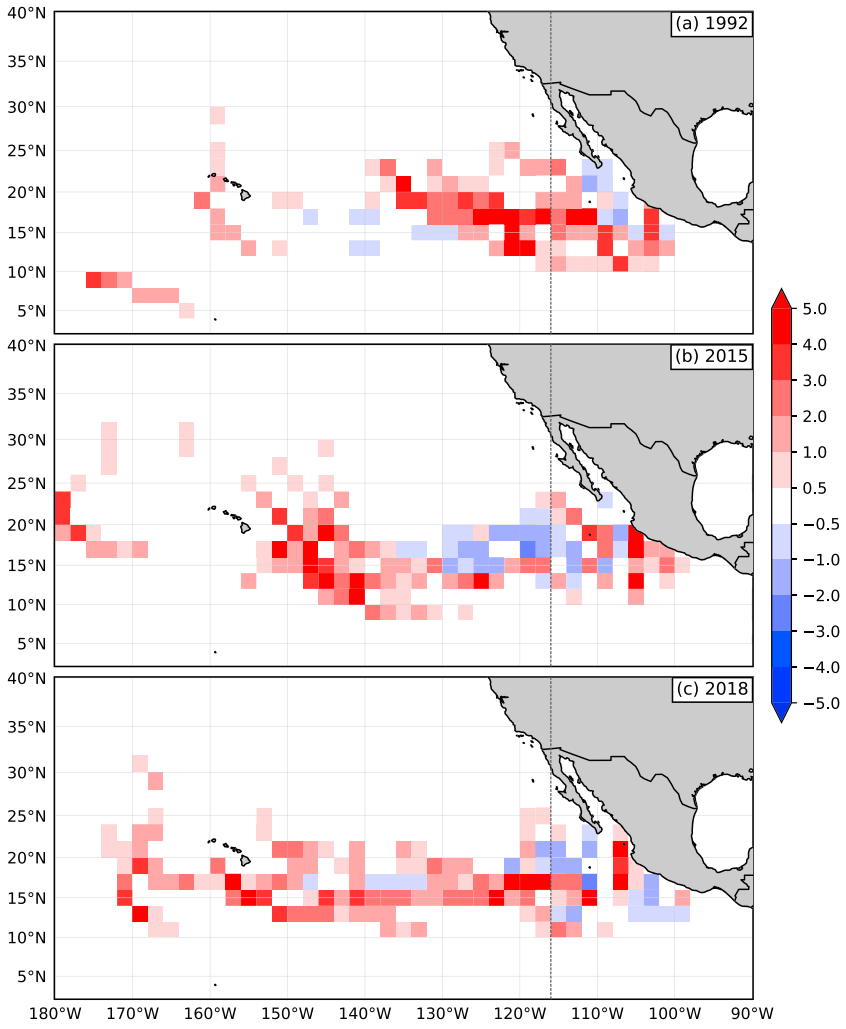

Figure 1. Two-degreeed cyclone energy anomalies (10^4 kt^2) relative to 1988–2017 during (a) 1992, (b) 2015, and (c) 2018. The vertical dotted line separates the Western Development Region and Eastern Development Region (116°W).

3. Activity in 2018 Compared with Past Active ENP Seasons

In 2018, the ENP (from the North American coast to 180°) produced 318×10^4 kt^2 of ACE. By contrast, 2015 produced 289×10^4 kt^2, only slightly less than the previous record of 294×10^4 kt^2 set in 1992. However, the spatial distribution of activity varies between these three seasons (Figure 1). The density of ACE within the eastern part of the basin was greater in 1992 than 2015 or 2018, whereas 2015 and 2018 produced more ACE within the western part of the basin.

Past work has shown a weak-to-nonexistent relationship between ENSO and ENP TC frequency (Whitney & Hobgood, 1997) when the full basin is evaluated. We divide the ENP into two regions: the Western Development Region (WDR; 180–116°W) and the Eastern Development Region (EDR; east of 116°W; e.g., Collins & Mason, 2000; Collins, 2007; Collins & Roache, 2011; Collins et al., 2016). The 2018 season produced slightly less ACE in the EDR than 2015 (78×10^4 kt^2 vs. 95×10^4 kt^2), but 2018 produced more ACE in the WDR (240×10^4 kt^2 vs. 194×10^4 kt^2; see Figure 2). Hereafter, all TC statistics focus on TCs located west of 116°W, or within the WDR.

A sharp increase in activity during August and September contributed to 2018's overall record-breaking WDR ACE (Figure 2a), dominated by Hurricanes Hector, Lane, Norman, and Olivia. Hector peaked as a strong category 4 hurricane (135 kt; 69.5 m/s) and maintained category 3 strength (≥100 kt) for over

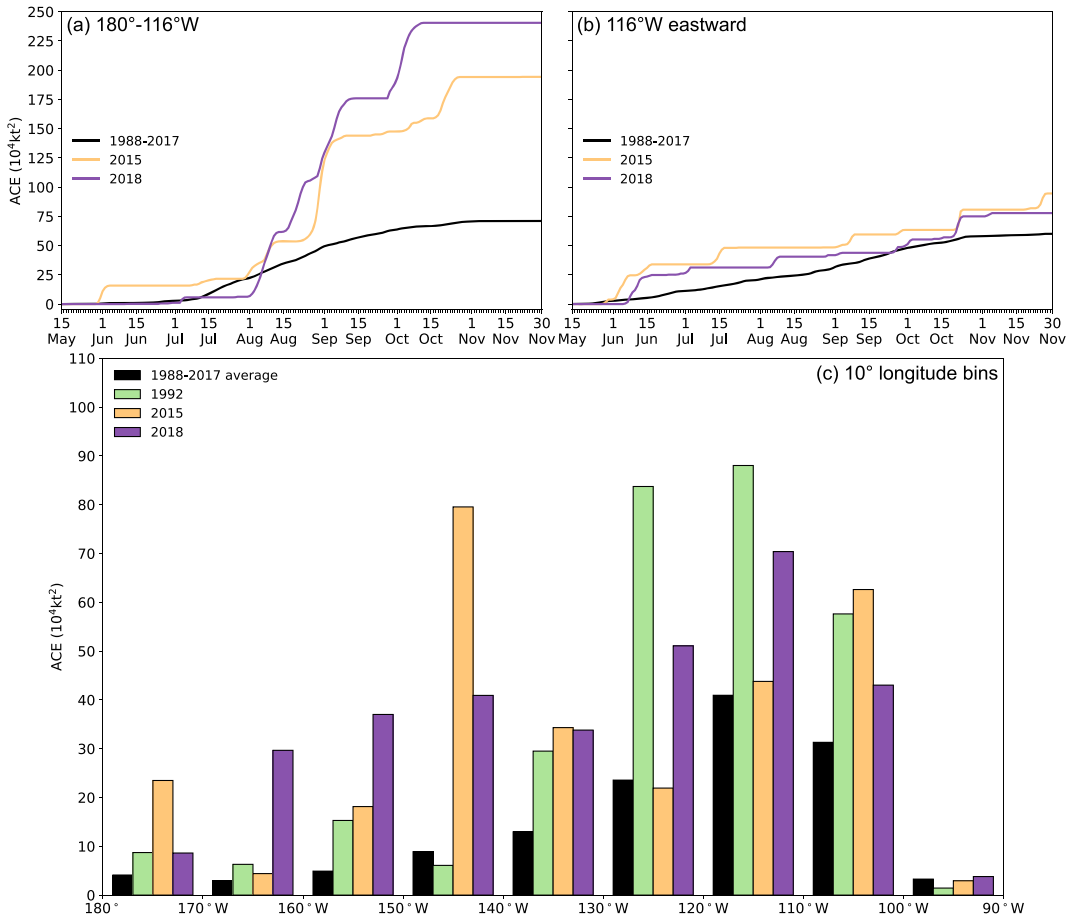

Figure 2. Cumulative accumulated cyclone energy (ACE; 10^4 kt^2) from 15 May to 30 November for 1988–2017 (black), 2015 (orange), and 2018 (purple) in the (a) Western Development Region and (b) Eastern Development Region. (c) Sum of all ACE (10^4 kt^2) generated within 10° longitude bins for 1988–2017 (black) and the 1992 (green), 2015 (orange), and 2018 (purple) seasons.

7 days, producing 50×10^4 kt^2 of ACE in the WDR alone. Hector generated the most ACE by an individual TC in the WDR since Hurricane John (49×10^4 kt^2) in 1994.

In 2018, 16 named storms spent part or all of their lifetimes within the WDR (≥34 kt), with nine of those reaching hurricane strength (≥64 kt) and seven reaching major hurricane strength (≥96 kt). More named storms (19) and hurricanes (10) but fewer major hurricanes (6) occurred in the WDR in 2015. Table S1 in the supporting information compares aggregate levels of TC activity in the WDR in 2018 and 2015. Despite fewer named TCs overall, the 2018 WDR storms attained higher intensities for longer periods of time compared with the 2015 WDR storms.

Among the top three WDR ACE years, 2015 produced the most ACE between 180° and 170°W and between 150° and 140°W, but 2018 was well above normal throughout the WDR and above normal in all 10° longitude bins (Figure 2c). These numbers imply most of the ENP basin was conducive for TCs at some point during the 2018 season. Note that the 1992 ENP hurricane season coincided with ENSO-neutral conditions after a strong El Niño event, and the bulk of 1992 activity occurred in the eastern half of the basin.

More TCs developed east of 116°W in 2018 than 2015, which is not surprising since El Niño events (e.g., 2015) can induce a westward shift in the ENP TC formation region. However, many of the 2018 EDR TCs crossed 116°W and entered the WDR. We hypothesize the increase in frequency of EDR TCs that subsequently entered the WDR contributed to higher ACE in 2018 because these storms were often already strong and/or intensifying as they crossed 116°W. In the next section, we investigate 2018 environmental conditions across the WDR.

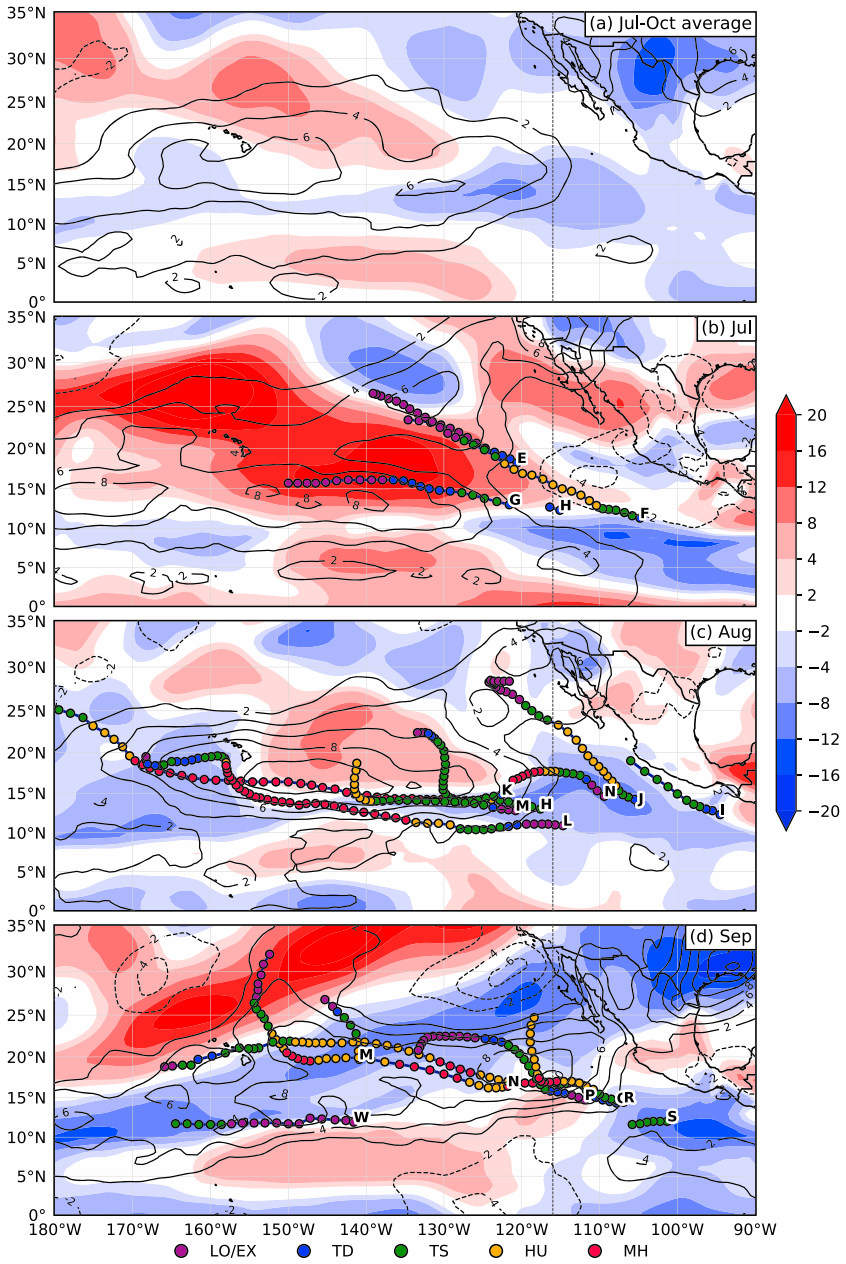

Figure 3. Anomalies (relative to 1998–2017) of 200-850-hPa vertical wind shear (kt; shaded) and total precipitable water (kg/m^2; contours) during (a) July–October 2018 and in (b) July 2018, (c) August 2018, and (d) September 2018, individually. Dots in panels (b)–(d) indicate 6-hourly tropical cyclone locations and intensities during each month. Letters denote the first storm location in the given month.

4. Environmental Conditions During 2018

An average of 96% of WDR ACE was produced during July–October over the 1988–2017 period; thus, our analyses focus on this time frame.

4.1. Climate Indices

ENSO-neutral conditions prevailed during July–September 2018. Niño 3.4 region (5°S to 5°N, 170–120°W) SST anomalies did not exceed the 0.5 °C threshold until October, and Multivariate ENSO Index values briefly peaked at 0.5 for August–September before decreasing again. Though El Niño can contribute to high ENP

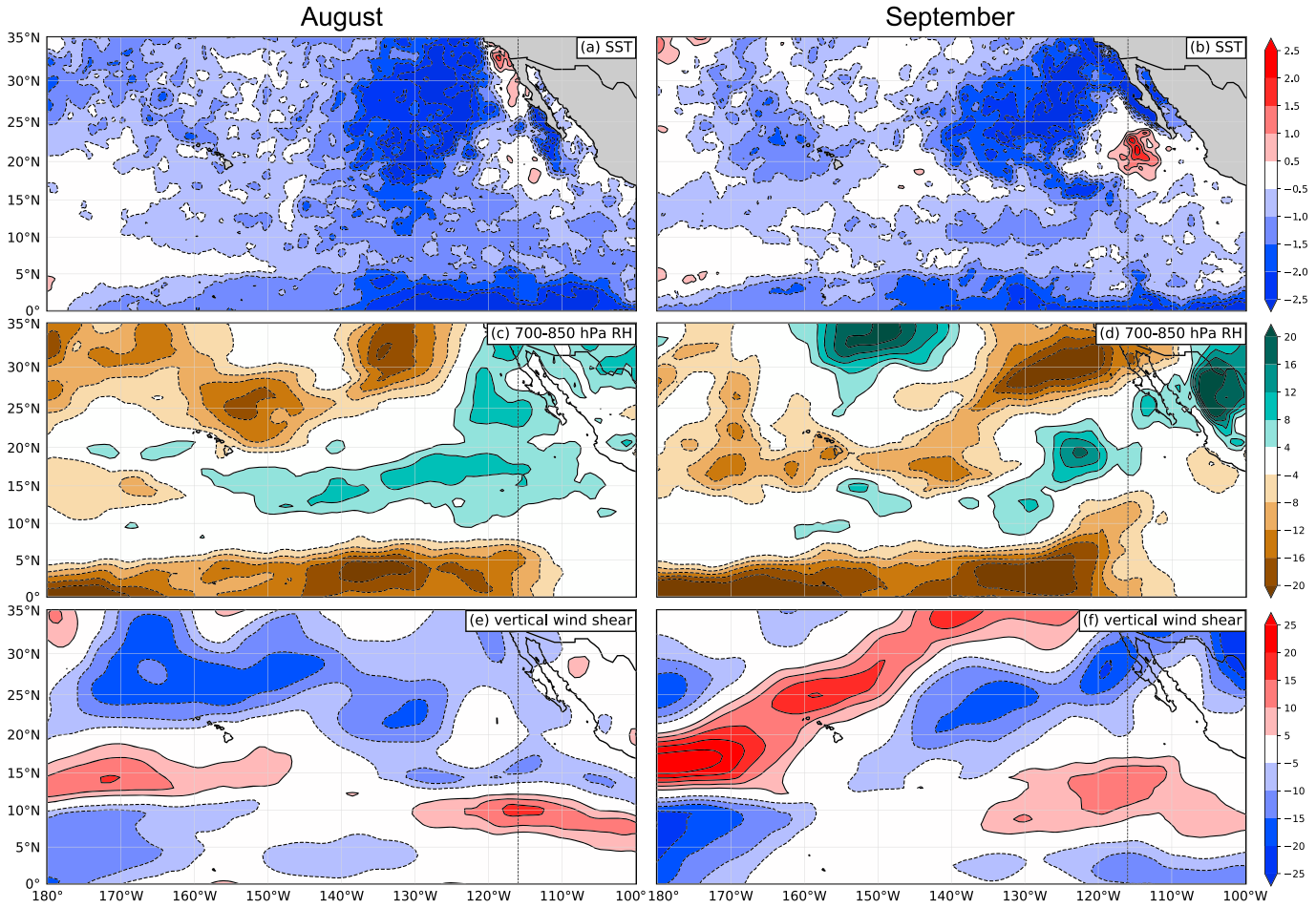

Figure 4. Differences between 2018 and 2015 during August (left column) and September (right column): (a and b) sea surface temperature (SST; °C), (c and d) 700-850-hPa relative humidity (%), and (e and f) 200-850-hPa vertical wind shear (kt). SSTs are provided by the NOAA OISST dataset, and relative humidity and vertical wind shear are provided by ERA-Interim.

activity (e.g., Collins et al., 2016), ENSO did not strongly contribute to the record-breaking 2018 season. Figure S1 shows a large spread in the generally positive correlation between ACE and ENSO.

The SST component of the PMM was strongly positive during July–October 2018. A positive PMM phase is associated with anomalously low pressure and anomalously weak trade winds in the ENP, both of which are favorable conditions for TC formation (Collins et al., 2016). Weak trade winds also reduce mixing and evaporation, thereby sustaining above-average SSTs. The SST component of the PMM showed a strong correlation with WDR ACE over the 1988–2017 period ($r = 0.49$), with higher PMM SST values corresponding to more WDR ACE. This relationship persisted in 2018, with a positive July–October PMM SST value of 1.2 standard deviations. This 2018 value was the third-highest July–October-averaged PMM value since 1988, trailing only 1992 and 1994. The above-average SSTs associated with this strong PMM signal likely supported EDR TCs crossing into the WDR and further strengthening.

The PDO can affect ENP TC activity (section 1), but it is strongly correlated with both the PMM and ENSO (Table S2). Since we restrict our analyses to 1988–2018 in this study, we focus on the PMM and ENSO given their shorter time scales of variability.

We next examine the predictors used in the diagnostic model proposed in Caron et al. (2015), who predict full-basin hurricane activity using Poisson regression and a combination of ENP relative SST (the difference between SST in the regions 15–30°N, 120–100°W and 30°S to 30°N, 0–360°) and SST in the North Atlantic subpolar gyre (50–70°N, 60–20°W) during July–September. We use July–October averages, since both predictors show slightly improved correlations when including October data. Using July–October 1988–2017

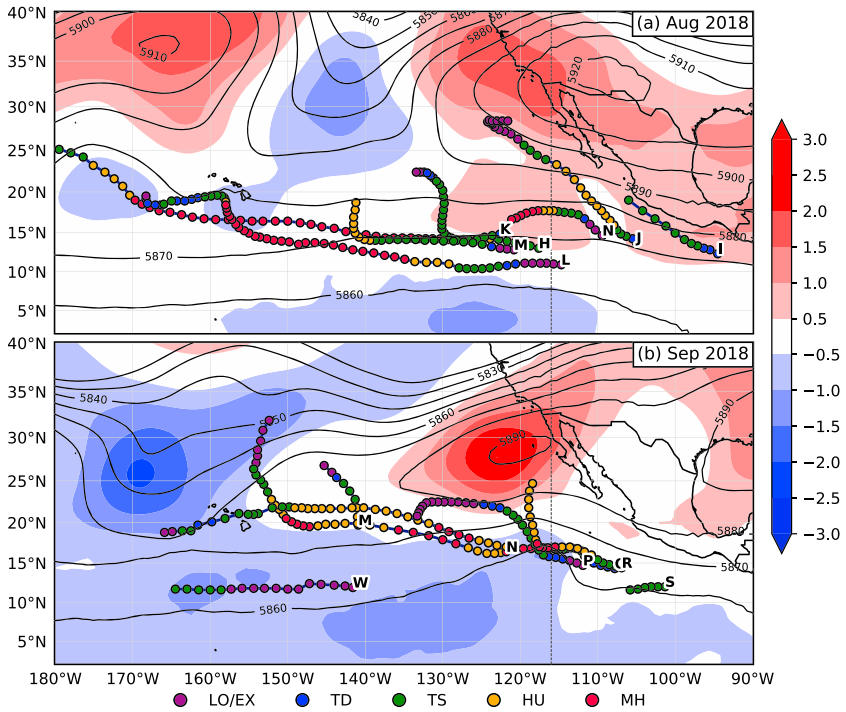

Figure 5. Five hundred-hectopascal geopotential height standard anomalies relative to 1988–2017 (shaded) and 500-hPa geopotential heights (m; contours) for (a) August 2018 and (b) September 2018. Dots indicate 6-hourly TC locations and intensities during each month. Letters denote the first storm location in the given month.

averaged OISST, ENP relative SST exhibits a strong correlation (r = 0.63) with ENP ACE, while North Atlantic subpolar gyre SST shows a strong *negative* correlation (r = −0.55). When combined in a simple linear regression model, the two parameters explain over 65% of the variability in 1988–2017 ENP ACE (r = 0.82). Each of these two predictors favored an active season in 2018, with 2018 having the fifth warmest July–October rank of ENP relative SST and the 10th coldest July–October rank of North Atlantic subpolar gyre SST since 1988. When both predictors are combined, the Caron et al. (2015) model called for 2018 to be the fourth most active season since 1988. Though this model did not predict the *most* active season on record, the combination of off-equatorial warmth in the ENP and a cold North Atlantic subpolar gyre likely contributed to the extremely active season. Caron et al. (2015) hypothesized that a cold North Atlantic subpolar gyre is associated with increased tropical Atlantic vertical wind shear and suppressed convection, with a concomitant reduction in ENP vertical wind shear and an increase in convection. Notably, the former full-basin ENP record holder for ACE (1992) coincided with the coldest July–October North Atlantic subpolar gyre from 1988 to 2018.

4.2. Large-Scale Conditions

In 2018, average July–October 200-850-hPa vertical wind shear was slightly below normal across much of the WDR (Figure 3a). Above-average values were largely explained by strong shear during the month of July (Figure 3b), likely driven by convectively suppressed phases of the MJO (discussed in more detail later in this section). Only one storm (Fabio) entered the WDR from the EDR in early July and subsequently weakened, while the other maintained tropical storm status for only 24 hr in late July (Gilma).

However, in August, the shear abated and moisture increased across much of the WDR (Figure 3c). A series of intense and long-lived TCs subsequently took advantage of this narrow band of below-average shear southeast and south of Hawaii, including Hector and Lane. During September, shear further decreased and above-normal moisture persisted (Figure 3d). The September decrease in shear may be related to a northward shift of the subtropical jet (Figure S2), resulting in a wide, relatively high-latitude band of

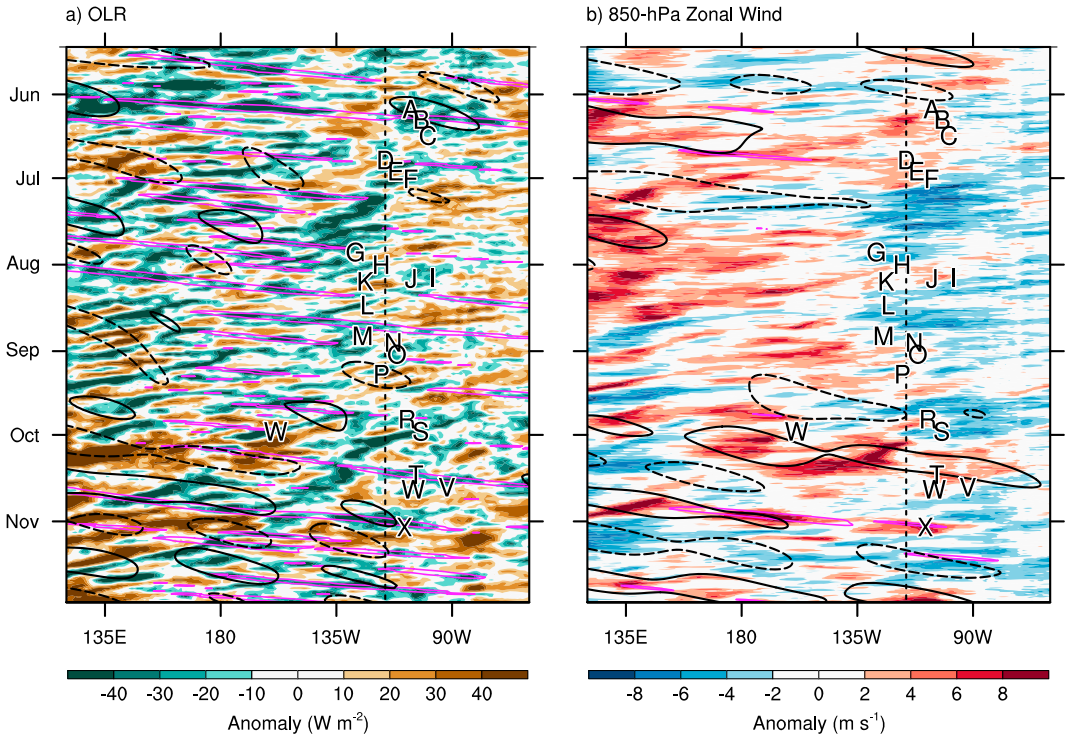

Figure 6. Longitude-time Hovmöller diagrams of average 5–15°N anomalous (a) outgoing longwave radiation (OLR; Schreck et al., 2018) and (b) 850-hPa zonal wind. Anomalies filtered for Kelvin waves are contoured in magenta at −10 W/m^2 and +2 m/s, and anomalies filtered for the Madden-Julian oscillation are contoured in black at ±10 W/m^2 (positive dashed) and ±2 m/s (negative dashed). Letters indicate tropical cyclone genesis time and genesis latitude. Vertical dashed line denotes 116°W. Shaded anomalies are relative to a 1981–2010 daily climatology.

below-average shear that extended northward to the Big Island of Hawaii. Again, multiple TCs traversed this low shear region, including Hurricanes Norman and Olivia (section 1).

Given the August–September 2018 burst of TC activity that exceeded 2015 levels (Figure 2a), we contrast these conditions to what occurred in 2015. With a strong El Niño in place, average 2015 SST exceeded average 2018 SST by 0.5–2 °C in both months (Figures 4a and 4b), and 2015 SST anomalies were much higher than 2018 (Figure S3). However, higher values of 700-850-hPa relative humidity were present in August 2018 across much of the basin between 10° and 20°N (Figure 4c), and vertical wind shear was lower in a large swath of the basin in both August and September 2018 (Figures 4e and 4f). As previously mentioned, the apparent northward shift in the subtropical jet likely supported lower shear in September 2018 compared with September 2015.

The average steering flow likely impacted how the large-scale environment affected overall WDR activity. In 2015, WDR TCs moved west-northwestward to northward (290–360°) 51% of the time, but 2018 WDR TCs did the same only 33% of the time. However, 2015 WDR TCs moved southwestward to west-northwestward (225–285°) 32% of the time, while 51% of 2018 WDR TCs did the same. An above-average subtropical ridge extending from North America into the eastern part of the basin, particularly in September (Figure 5), likely enhanced the westward steering flow and thus enabled 2018 TCs to remain in more favorable environments, including high SSTs influenced by the strong PMM (section 4.1). The subtropical ridge in August and September 2018 was stronger than in 2015, which supports the observed TC motion patterns in each season (Figure S4). Though beyond the scope of this paper, future work should examine the relationship between the ridge associated with the North American monsoon and ENP TC activity, particularly its association with intraseasonal variability of ENP TC activity.

The simultaneous existence of above-average moisture and below-average vertical wind shear in both August and September 2018 along most TC tracks appears to have contributed to the increase in WDR activity in those months. A weakening of upper-level winds along these TC tracks (Figure S2)

likely drove part of the reduction in wind shear and may have generated improved TC outflow for stronger storms.

In 2015, multiple active periods were separated by days to weeks of low-to-nonexistent TC activity (Figure 2): 95% of 2015 WDR ACE occurred between 1 June and 27 October. These active periods often coincided with convectively active MJO phases (Collins et al., 2016). In 2018, most TC activity occurred within a *10-week* time span: 95% of WDR ACE was produced between 3 August and 12 October. The suppressed convection and easterly anomalies that inhibited TC activity during July 2018 were associated with an eastward-propagating suppressed-convective MJO signal from the western Pacific (Figure 6, dashed lines). However, the MJO was generally inactive during the period of peak 2018 TC activity, which might explain the prolonged and continuous nature of that activity. In the absence of a coherent MJO, several atmospheric Kelvin waves propagated across the Pacific (Figure 6a, magenta contours) and may have fostered the development of several ENP TCs, including Kristy and Miriam in the WDR.

5. Conclusions

This study investigates 2018 TC activity west of 116°W in the ENP (the WDR), which broke the WDR ACE record set in 2015. A weak El Niño event did not manifest until late in the hurricane season, yet above-average SSTs between 10° and 20°N (a positive PMM phase) combined with above-average moisture and below-average shear—particularly in August and September—contributed to record-breaking WDR TC activity. Cold waters in the subpolar North Atlantic likely also contributed to high ENP TC activity. Many TCs that developed east of 116°W encountered favorable conditions as they translated westward and entered the WDR, where they further strengthened and persisted.

ENSO did not strongly contribute to the record amount of 2018 WDR ACE. Though several studies have investigated the impact of El Niño and La Niña on ENP TC activity, additional research is needed on the relationship between ENP TC activity and ENSO-neutral conditions. The extremely active 2018 ENP hurricane season also highlights the need for more research into the PMM's influence on ENP TC activity.

Acknowledgments
All data included in this study are freely available from the NOAA and UCAR websites cited in the text. Many figures were produced using Cartopy (https://scitools.org.uk/cartopy/docs/latest/). The authors thank Dr. Suzana Camargo and two anonymous reviewers for their valuable feedback on earlier versions of this manuscript. K. Wood was supported by the Mississippi State University Office of Research and Economic Development. P. Klotzbach acknowledges funding from the G. Unger Vetlesen Foundation. C. Schreck was supported by NOAA through the Cooperative Institute for Climate and Satellites – North Carolina under Cooperative Agreement NA14NES432003.

References

Bell, G. D., Halpert, M. S., Schnell, R. C., Higgins, R. W., Lawrimore, J., Kousky, V. E., et al. (2000). Climate assessment for 1999. *Bulletin of the American Meteorological Society*, *81*(6), S1–S50. https://doi.org/10.1175/1520-0477(2000)81[s1:CAF]2.0.CO;2

Blake, E. S., Gibney, E. J., Brown, D. P., Mainelli, M., Franklin, J. L., & Kimberlain, T. B. (2009). *Tropical cyclones of the eastern North Pacific basin, 1949–2006*, *Historical Climatology Series* (Vol. 6-5, p. 162). Asheville, NC: National Climatic Data Center.

Brennan, M. J., 2019: Hurricane Willa. National Hurricane Center Tropical Cyclone Report, NHC, *29* pp. https://www.nhc.noaa.gov/data/tcr/EP242018_Willa.pdf.

Camargo, S. J., Robertson, A. W., Barnston, A. G., & Ghil, M. (2008). Clustering of eastern North Pacific tropical cyclone tracks: ENSO and MJO effects. *Geochemistry, Geophysics, Geosystems*, *9*, Q06V05. https://doi.org/10.1029/2007GC001861

Caron, L.-P., Boudreault, M., & Camargo, S. J. (2015). On the variability and predictability of eastern North Pacific tropical cyclone activity. *Journal of Climate*, *28*, 9678–9696. https://doi.org/10.1175/JCLI-D-15-0377.1

Chiang, J. C. H., & Vimont, D. J. (2004). Analogous Pacific and Atlantic meridional modes of tropical atmosphere–ocean variability. *Journal of Climate*, *17*(21), 4143–4158. https://doi.org/10.1175/JCLI4953.1

Collins, J. M. (2007). The relationship of ENSO and relative humidity to interannual variations of hurricane frequency in the North-East Pacific ocean. *Papers of the Applied Geography Conferences*, *30*, 324–333.

Collins, J. M., Klotzbach, P. J., Maue, R. N., Roache, D. R., Blake, E. S., Paxton, C. H., & Mehta, C. A. (2016). The record-breaking 2015 hurricane season in the eastern North Pacific: An analysis of environmental conditions. *Geophysical Research Letters*, *43*, 9217–9224. https://doi.org/10.1002/2016GL070597

Collins, J. M., & Mason, I. M. (2000). Local environmental conditions related to seasonal tropical cyclone activity in the northeast Pacific basin. *Geophysical Research Letters*, *27*(23), 3881–3884. https://doi.org/10.1029/2000GL011614

Collins, J. M., & Roache, D. R. (2011). The 2009 hurricane season in the eastern North Pacific basin: An analysis of environmental conditions. *Monthly Weather Review*, *139*(6), 1673–1682. https://doi.org/10.1175/2010MWR3538.1

Dee, D. P., Uppala, S. M., Simmons, A. J., Berrisford, P., Poli, P., Kobayashi, S., et al. (2011). The ERA-Interim reanalysis: Configuration and performance of the data assimilation system. *Quarterly Journal of the Royal Meteorological Society*, *137*, 553–597. https://doi.org/10.1002/qj.828

Irwin, R. P., & Davis, R. (1999). The relationship between the Southern Oscillation Index and tropical cyclone tracks in the eastern North Pacific. *Geophysical Research Letters*, *26*(15), 2251–2254. https://doi.org/10.1029/1999GL900533

Jien, J. Y., Gough, W. A., & Butler, K. (2015). The influence of El Niño-Southern Oscillation on tropical cyclone activity in the eastern North Pacific basin. *Journal of Climate*, *28*(6), 2459–2474. https://doi.org/10.1175/JCLI-D-14-00248.1

Kiladis, G. N., Straub, K. H., & Haertel, P. T. (2005). Zonal and vertical structure of the Madden–Julian oscillation. *Journal of the Atmospheric Sciences*, *62*(8), 2790–2809. https://doi.org/10.1175/JAS3520.1

Kiladis, G. N., Wheeler, M. C., Haertel, P. T., Straub, K. H., & Roundy, P. E. (2009). Convectively coupled equatorial waves. *Reviews of Geophysics*, *47*, RG2003. https://doi.org/10.1029/2008RG000266

Klotzbach, P. J., & Landsea, C. W. (2015). Extremely intense hurricanes: Revisiting Webster et al. (2005) after 10 years. *Journal of Climate*, *28*(19), 7621–7629. https://doi.org/10.1175/JCLI-D-15-0188.1

Landsea, C. W., & Franklin, J. L. (2013). Atlantic hurricane database uncertainty and presentation of a new database format. *Monthly Weather Review*, *141*(10), 3576–3592. https://doi.org/10.1175/MWR-D-12-00254.1

Mantua, N. J., Hare, S. R., Zhang, Y., Wallace, J. M., & Francis, R. C. (1997). A Pacific interdecadal climate oscillation with impacts on salmon production. *Bulletin of the American Meteorological Society*, *78*(6), 1069–1079. https://doi.org/10.1175/1520-0477(1997)078<1069:APICOW>2.0.CO;2

Patricola, C. M., Saravanan, R., & Chang, P. (2017). A teleconnection between Atlantic sea surface temperature and eastern and central North Pacific tropical cyclones. *Geophysical Research Letters*, *44*, 1167–1174. https://doi.org/10.1002/2016GL071965

Raga, G. B., Bracamontes-Ceballos, B., Farfán, L. M., & Romero-Centeno, R. (2013). Landfalling tropical cyclones on the Pacific coast of Mexico: 1850–2010. *Atmosfera*, *26*(2), 209–220. https://doi.org/10.1016/S0187-6236(13)71072-5

Schreck, C. J., Lee, H.-T., & Knapp, K. R. (2018). HIRS outgoing longwave radiation—Daily climate data record: Application toward identifying tropical subseasonal variability. *Remote Sensing*, *10*, 1325. https://doi.org/10.3390/rs10091325

Smith, D. M., Eade, R., Dunstone, N. J., Fereday, D., Murphy, J. M., Pohlmann, H., & Scaife, A. A. (2010). Skillful multi-year predictions of Atlantic hurricane frequency. *Nature Geoscience*, *3*, 846–849. https://doi.org/10.1038/ngeo1004

Wang, C., & Lee, S.-K. (2009). Co-variability of tropical cyclones in the North Atlantic and the eastern North Pacific. *Geophysical Research Letters*, *36*, L24702. https://doi.org/10.1029/2009GL041469

Whitney, L. D., & Hobgood, J. (1997). The relationship between sea surface temperature and maximum intensities of tropical cyclones in the eastern North Pacific. *Journal of Climate*, *10*(11), 2921–2930. https://doi.org/10.1175/1520-0442(1997)010<2921:TRBSST>2.0.CO;2

Wolter, K., & Timlin, M. S. (1998). Measuring the strength of ENSO events—How does 1997/98 rank? *Weather*, *53*(9), 315–324. https://doi.org/10.1002/j.1477-8696.1998.tb06408.x

Wood, K. M., & Ritchie, E. A. (2013). An updated climatology of tropical cyclone impacts on the southwestern United States. *Monthly Weather Review*, *141*(12), 4322–4336. https://doi.org/10.1175/MWR-D-13-00078.1